304

NASA TM X-50066

48

N63 82665

MTP-M-G&C-60-14
December 13, 1960

GEORGE C. MARSHALL SPACE FLIGHT CENTER

HUNTSVILLE, ALABAMA

TWO METHODS OF SPACE VEHICLE ATTITUDE CONTROL EMPLOYING FLYWHEEL REACTION TORQUES

by

Paul T. Golley

NASA FILE COPY

PLEASE RETURN TO CODE ETL
OFFICE OF TECHNICAL INFORMATION
AND EDUCATIONAL PROGRAMS
NATIONAL AERONAUTICS
AND SPACE ADMINISTRATION

NOTICE

This document was prepared for NASA internal use, and the information contained herein is subject to change.

NATIONAL AERONAUTICS AND SPACE ADMINISTRATION

REC - Capt C. H. Gould

ABSTRACT

This report presents a nonlinear system of attitude control which employs the reaction torques of accelerated flywheels as a restoring agent. The system consists of three cylindrical flywheels, one in each of three mutually perpendicular axes. Each flywheel is powered by a separate motor; however, the control methods developed here are equally applicable to a spherical flywheel driven by a system of three torquers. To facilitate the investigation, a single axis is examined, neglecting interaxis coupling.

In both methods, the motor begins compensation when a certain attitude deadband is exceeded. In the first method, the motor "on-time" needed to compensate a disturbing impulse is determined by the angular velocity of the vehicle which existed at the time of motor activation. In the second method, the motor "on-time" is determined by employing instantaneous attitude and velocity information.

Theoretical and analog results are presented for comparison. The results are in the form of phase plane plots, and comparison of the theoretical with the analog plots shows complete agreement.

Although both control methods are feasible, the second has decided advantages over the first in that it uses less power, requires less switching, and provides a greater range in which certain parameters can vary.

December 13, 1960 MTP-M-G&C-60-14

TWO METHODS OF SPACE VEHICLE ATTITUDE CONTROL EMPLOYING FLYWHEEL REACTION TORQUES

by

Paul T. Golley

GUIDANCE & CONTROL DIVISION
GEORGE C. MARSHALL SPACE FLIGHT CENTER
HUNTSVILLE, ALABAMA

TABLE OF CONTENTS

	Page
INTRODUCTION.	1
EQUATIONS OF TORQUE	1
METHOD I.	2
METHOD II	5
RESULTS.	6
CONCLUSIONS	7
APPENDIX.	8

DEFINITIONS OF SYMBOLS

Symbol	Definition	Unit
ϕ	Angular displacement of vehicle	radians
ϕ_s	Angular velocity at the time the motor switches off	radians
$\dot{\phi}$	Angular velocity of the vehicle	rad/sec
$\dot{\phi}_i$	Angular velocity at the time the motor switches on	rad/sec
$\dot{\phi}_s$	Angular velocity at the time the motor switches off	rad/sec
$\dot{\phi}_{lim}$	Angular velocity at the time of switch-on while the system is in the limit cycle	rad/sec
$\ddot{\phi}$	Angular acceleration of the vehicle	rad/sec^2
$\ddot{\phi}_m$	Constant acceleration provided by the motor	rad/sec^2
$\ddot{\alpha}$	Angular acceleration of the flywheel	rad/sec^2
σ	Part of $\ddot{\phi}_m$ which is consumed by losses	percent
I_v	Moment of inertia of the vehicle	m-kg-sec^2
I_f	Moment of inertia of the flywheel	m-kg-sec^2
t_c	Constant interval of time	seconds
t_{on}	Length of time the motor operates	seconds
K_1	Constant coeficient of velocity in on-time equation	seconds^2
K_2	Constant coefficient of displacement in switch-off equation	rad/sec^2

LIST OF ILLUSTRATIONS

Figure		Page
1.	Flywheel Control System (One Axis)	9
2.	Motor Characteristics	10
3.	Phase Plane Plot of Characteristic Performance	11
4.	Theoretical Phase Plane Plot of Method I	12
5.	Block Diagram of Method I (One Axis)	13
6.	Theoretical Phase Plane Plot of Method II	14
7.	Block Diagram of Method II (One Axis)	15
8-15.	Analog Simulation Phase Plane Plots	16-23
16.	Definition of Displacements	24

INTRODUCTION

Presented here are two methods of control which employ the reaction torque of an accelerated flywheel as a restoring agent. Three cylindrical flywheels may be employed, one in each of three mutually perpendicular axes, or one spherical flywheel with three mutually perpendicular torquers. The control methods developed here are for cylindrical flywheels, each driven by its own motor; however, the entire report is equally applicable to a system of three torquers and a spherical flywheel.

EQUATIONS OF TORQUE

The vehicle and its flywheels compose a system in which the sum of the torques about the center of mass must equal zero to maintain a specified attitude. The investigation is simplified by considering only one axis which would (neglecting interaxis coupling), be typical of either of the three mutually perpendicular axes in the vehicle. By assuming no external torques, torque in one axis may be expressed as the product of the moment of inertia and angular acceleration. The expression relating the torques is

$$I_v\ddot{\phi} - I_f\ddot{\alpha} = 0$$

where I_v and I_f are the moments of inertia of the vehicle and the flywheel respectively, and where $\ddot{\phi}$ and $\ddot{\alpha}$ are the angular acceleration of the vehicle and flywheel respectively. If the initial conditions are considered zero, the displacements, velocities, and accelerations of the vehicle differ only by the scale factor, $\frac{I_f}{I_v}$, from the displacements, velocities, and accelerations of the flywheel. Specifically:

$$\phi = \frac{I_f}{I_v}\alpha$$

$$\dot{\phi} = \frac{I_f}{I_v}\dot{\alpha}$$

$$\ddot{\phi} = \frac{I_f}{I_v}\ddot{\alpha}$$

Figure 1 shows the basic layout of one axis of the flywheel system which consists of a flywheel, a motor to drive the wheel, a control computer, an attitude sensor, and a power supply. The computer contains gate circuitry and an on-off type power amplifier to operate the motor. The on-off operation of the system requires a deadband within which the attitude of the vehicle is allowed to drift.

Figure 2 shows the motor characteristics. The speed versus torque plot shows that the motor torque is limited, which reduces the maximum power capacity requirement of the motor amplifier, because the starting peak of the motor current is eliminated. The speed versus time plot shows that due to the torque limiting, the motor acts like an integrator up to 85 percent of maximun speed. The effects of other motor characteristics on control will be discussed later.

Any rotation of the flywheel is opposed by friction. Viscous friction is considered to be sufficiently small to be neglected. The coulomb friction iron losses, etc., which exist, can be expressed as a constant torque opposing the rotation of the flywheel. The acceleration due to losses is written as a part of the motor acceleration, $\sigma\ddot{\phi}_m$.

Physically there are three possible combinations of acceleration:

1. $(1-\sigma)\ddot{\phi}_m$ With voltage on and motor speed increasing
2. $(1+\sigma)\ddot{\phi}_m$ With voltage on and motor speed decreasing
3. $\sigma\ddot{\phi}_m$ With voltage off and motor speed decreasing

Two control methods are discussed. They are similar in that both start the motor when the deadband is exceeded. They differ in that the first method determines the motor on-time by employing the velocity with which the deadband is exceeded, while the second method switches off the motor by comparing instantaneous attitude and velocity information.

METHOD I

In Method I, the motor on-time varies thus:

$$t_{on} = K_1 \left| \dot{\phi}_i \right| + t_c \qquad 1.0$$

This equation evolved in the following manner:

It was first chosen that

$$t_{on} = K_1 \left| \dot{\phi}_i \right| \qquad 1.1$$

where $\dot{\phi}_i$ is the velocity at the time of switch-on.

The equation describing the change in vehicle velocity for the motor on-time is

$$(1-\sigma)\ddot{\phi}_m t_{on} = \left|\dot{\phi}_s\right| + \left|\dot{\phi}_i\right| \qquad 1.2$$

where $\dot{\phi}_s$ is the velocity at switch-off, and $\ddot{\phi}_m$ is the magnitude of the constant acceleration of the motor.

Combining Equations 1.1 and 1.2 results in

$$K_1(1-\sigma)\ddot{\phi}_m - 1 = \frac{\left|\dot{\phi}_s\right|}{\left|\dot{\phi}_i\right|} \qquad 1.3$$

The system is stable when $\dot{\phi}_s$ is of opposite sign and is less in magnitude than $\dot{\phi}_i$:

$$-1 < \frac{\dot{\phi}_s}{\dot{\phi}_i} < 0$$

or:

$$1 > \frac{\dot{\phi}_s}{\dot{\phi}_i} > 0$$

Therefore:

$$\frac{2}{(1-\sigma)\ddot{\phi}_m} > K_1 > \frac{1}{(1-\sigma)\ddot{\phi}_m} \qquad 1.4$$

Until now, the effects of losses during motor off-time have been neglected. If K_1 is chosen to satisfy

$$K_1 > \frac{1+\sqrt{\sigma}}{(1-\sigma)\ddot{\phi}_m} \qquad 1.5$$

(see Appendix)

(which accounts for losses during motor off-time), the on-time is sufficient to arrest the disturbing velocity and drive the vehicle attitude back into the deadband, as shown by the solid curve in the phase plane plot of Figure 3. Point A shows the velocity resulting from a disturbance. At B (the deadband) the motor is switched on. At C, the motor has arrested the disturbing velocity. Further motor on-time provides a velocity which decreases the attitude angle to D, where the motor is switched off. During the period after D, the acceleration caused by the existing motor losses decreases the velocity. With sufficient velocity at D, the deadband will be reached before the opposing acceleration can change the sign of the velocity. The existing velocity, at E, can be considered a new disturbance and the cycle as described is repeated. The motor on-time under this condition will finally reach a minimum which is determined by the system lag, neglected in Equation 1.1. This would lead to a relatively high repetitive cycle, which is undesirable from the

point of reliability.

To prevent such undesirable conditions, a constant time t_c, which is larger than the inherent system lag, is added in Equation 1.1, resulting in

$$\frac{2}{(1-\sigma)\ddot{\phi}_m} > K_1 + \frac{t_c}{|\dot{\phi}_i|} > \frac{1+\sqrt{\sigma}}{(1-\sigma)\ddot{\phi}_m} \qquad 1.6$$

The lower and upper limits between stable and unstable operation are then defined by:

$$K_1 + \frac{t_c}{|\dot{\phi}_i|} = \frac{1+\sqrt{\sigma}}{(1-\sigma)\ddot{\phi}_m} \qquad 1.7$$

$$K_1 + \frac{t_c}{|\dot{\phi}_i|} = \frac{2}{(1-\sigma)\ddot{\phi}_m} \qquad 1.8$$

Solving for $\dot{\phi}_1$ in Equation 1.8 yields the limit cycle velocity,

$$\dot{\phi}_{1im} = \frac{t_c(1-\sigma)\ddot{\phi}_m}{2-(1-\sigma)\ddot{\phi}_m K_1} \qquad 1.9$$

Although the equations thus far contain only $(1-\sigma)\ddot{\phi}_m$ terms, they are equally applicable when control requires the $(1+\sigma)\ddot{\phi}_m$ term, with the exception of the limit cycle where only the term $(1-\sigma)\ddot{\phi}_m$ is valid (Eq 1.9).

The amplitude and period of the limit cycle are functions of the motor acceleration, the deadband width, and the motor losses. While the acceleration and the deadband width can be predetermined, the effects of losses in the absence of gravity must be estimated.

Assuming that the acceleration due to losses is considerably less than the estimated value, the restoring velocity at Point D of Figure 3 would result in an attitude displacement exceeding the deadband on the left side of the phase plane plot. This will not lead to an unstable behavior (see the dotted line in Fig 3). However, if the losses are considerably greater than the preset value, the velocity at D would not be sufficient to restore the attitude into the deadband, and control would be lost.

To avoid possible loss of control, the motor is switched on for a predetermined constant time interval whenever the velocity changes sign and the attitude is still outside the deadband, as indicated by the dot-dash line in Figure 3.

Figure 4 is a theoretical phase plane plot of Method I performance, showing the complete correction of a single disturbance, including the limit cycle (points KLMK).

Figure 5 is a block diagram of Method I logic circuitry, most of which is self-explanatory. Notice that only the absolute value of velocity is necessary to determine the instant of motor switch-off, because the cut-off equation generator sends an "off" signal to both motor switches, deactivating whichever one was activated. The items in the dashed area are necessary if the estimate of σ is quite inaccurate, or if a disturbance should occur while the motor is activated.

METHOD II

In Method II, the motor switch-off occurs in such a manner that disturbances are damped directly to zero without overshoot (Fig 6).

The following expression describes the motion of the vehicle in terms of ϕ and $\dot{\phi}$, while under the influence of the constant acceleration due to losses, $\sigma\ddot{\phi}_m$:

$$\Delta\phi = 1/2 \left[\frac{(\dot{\phi})^2}{\sigma\ddot{\phi}_m}\right] \qquad 2.1$$

This is the equation of a parabola with its vertex at the origin if $\Delta\phi$ is the attitude error ϕ. The equation can be arranged thus:

$$2(\sigma\ddot{\phi}_m)\phi - (\dot{\phi})^2 = 0 \qquad 2.2$$

or

$$K_2\phi - (\dot{\phi})^2 = 0 \qquad 2.3$$

There exists a multitude of combinations of ϕ and $\dot{\phi}$ which will satisfy the equation. If the motor switches off when one of these combinations exists, the vehicle attitude will follow the parabola to zero attitude because the acceleration due to losses begins acting as soon as the motor is switched off.

Figure 6 shows that the switch-off equation might be satisfied at some time before the attitude reaches Point C in the diagram which would not result in a velocity toward zero. Therefore, the equation is not employed until the velocity has changed sign once. Once switched off, the motor cannot be switched on again until another velocity sign change occurs, or until the attitude is within the deadband. The latter provision enables the system to maintain control even if σ is underestimated, or if disturbances occur while the attitude is outside the deadband. The system behavior under these conditions is shown in Figures 13 and 14

which are obtained through analog simulation of the system. Since either of these conditions might change the sign of the velocity, the motor would switch on to re-establish a velocity toward zero attitude.

Once a disturbance has been corrected, and the attitude has been brought within the deadband, the system settles down to the limit cycle (points EFGE in Fig. 6). The acceleration due to losses drives the vehicle attitude out of the deadband at F, causing the control action to be repeated. The amplitude and period of the limit cycle oscillation are determined by the amount of acceleration due to losses. The nominal condition, which is estimated and preset before launch, would exist when the minimum attitude error during the limit cycle just reaches zero (i.e., the parabola described by the switch-off equation has its vertex exactly at zero attitude).

Figure 7 is a block diagram of Method II logic circuitry. Only the absolute values of ϕ and $\dot{\phi}$ must be known since the comparator sends an off-signal to both motor switches. In the comparator the difference between the absolute values of $K_2\phi$ and $\dot{\phi}^2$ is detected. When Equation 2.3 is satisfied, the motor is switched off. Equation 2.3 is then rewritten

$$K_2 \left| \phi_s \right| - (\dot{\phi}_s)^2 = 0 \qquad 2.4$$

and is called the switch-off equation, where ϕ_s and $\dot{\phi}_s$ are the desired combination of displacement and velocity for switch-off.

RESULTS

Both control methods were tested by analog simulation and the results are presented in phase plane plots.

Three plots show simulated Method I performance:

Figure 8.	When losses are nominal
Figure 9.	When losses are less than nominal
Figure 10.	When losses are greater than nominal

Five plots show simulated Method II performance:

Figure 11.	When losses are nominal
Figure 12.	When losses are less than nominal
Figure 13.	When losses are greater than nominal
Figure 14.	When additional disturbances occur before the previous one is damped
Figure 15.	Calculated plot of the performance when additional disturbances occur before the previous one is damped

In some of the plots there are smaller limit cycles within the normal limit cycle. These result from initial velocities less than the maximum limit cycle velocity.

Notice that the vehicle speed can never exceed the initial value, because the flywheel can only come to rest and losses cannot slow it down further.

Under actual operating conditions, it would be unlikely for this situation to occur since the flywheel would normally have a considerable velocity as the result of compensating part of the initial separation disturbance. However, if disturbances occur in such a sequence as to produce this condition, it can be seen by the plots that the system reacts favorably.

The fact that only losses which are expressed as a constant acceleration have been considered, and that the motor presently under consideration is torque-limited, simplifies the investigation, because in the phase plane plots, the angular velocity versus the angular displacement is parabolic. If viscous friction is included, and/or a different motor characteristic is considered, the obtained curves would deviate from the parabolic shape. The effect on control would be very slight. Failing to consider these two aspects would have the same effect as an inaccurate estimate of σ , which has already been discussed.

CONCLUSIONS

Either of the two methods investigated will provide satisfactory control. There are several reasons, however, which make Method II more favorable. In Method II, the disturbances (particularly larger ones) are damped far more rapidly than in Method I, requiring less switching and power, thus providing a saving in weight and reliability. The magnitude of the limit cycle displacement in Method II is inversely proportional to the acceleration due to losses, while in Method I the magnitude of the limit cycle is more than just an inverse function of losses. Thus Method II provides a greater range in which losses can vary and still return the attitude to the deadband with one sequence of motor operation.

APPENDIX

To be stable (with losses considered), the motor must remain activated for a time sufficient to provide a velocity toward zero attitude which will not be overcome by the acceleration due to losses before the attitude is within the deadband.

The right hand term of the inequality expressed in Equation 1.4 must then be modified by some amount which accounts for these losses. Figure 16 is a phase plane plot showing the correction of a disturbance where the motor stayed on long enough to provide a velocity back toward zero, so that the attitude just reaches the deadband before the acceleration due to losses changes the sign of the velocity. Equating the displacements labeled in the plot:

$$\phi_1 = \phi_2 - \phi_3 \tag{A}$$

The equation of motion of a body subject to a constant acceleration is:

$$\Delta\phi = \frac{(\dot{\phi})^2}{2\ddot{\phi}} \tag{B}$$

Combining Equations B and A, and applying the accelerations which occur in the phase plane plot results in:

$$\frac{(\dot{\phi}_i)^2}{2(1-\sigma)\ddot{\phi}_m} = \frac{(\dot{\phi}_s)^2}{2(1-\sigma)\ddot{\phi}_m} + \frac{(\dot{\phi}_s)^2}{2\sigma\ddot{\phi}_m} \tag{C}$$

Solving Equation C for the velocity ratio yields:

$$\frac{\dot{\phi}_s}{\dot{\phi}_i} = \sqrt{\sigma} \tag{D}$$

Whereupon Equation 1.4 becomes:

$$K_1 > \frac{1 + \sqrt{\sigma}}{(1-\sigma)\ddot{\phi}_m} \tag{1.5}$$

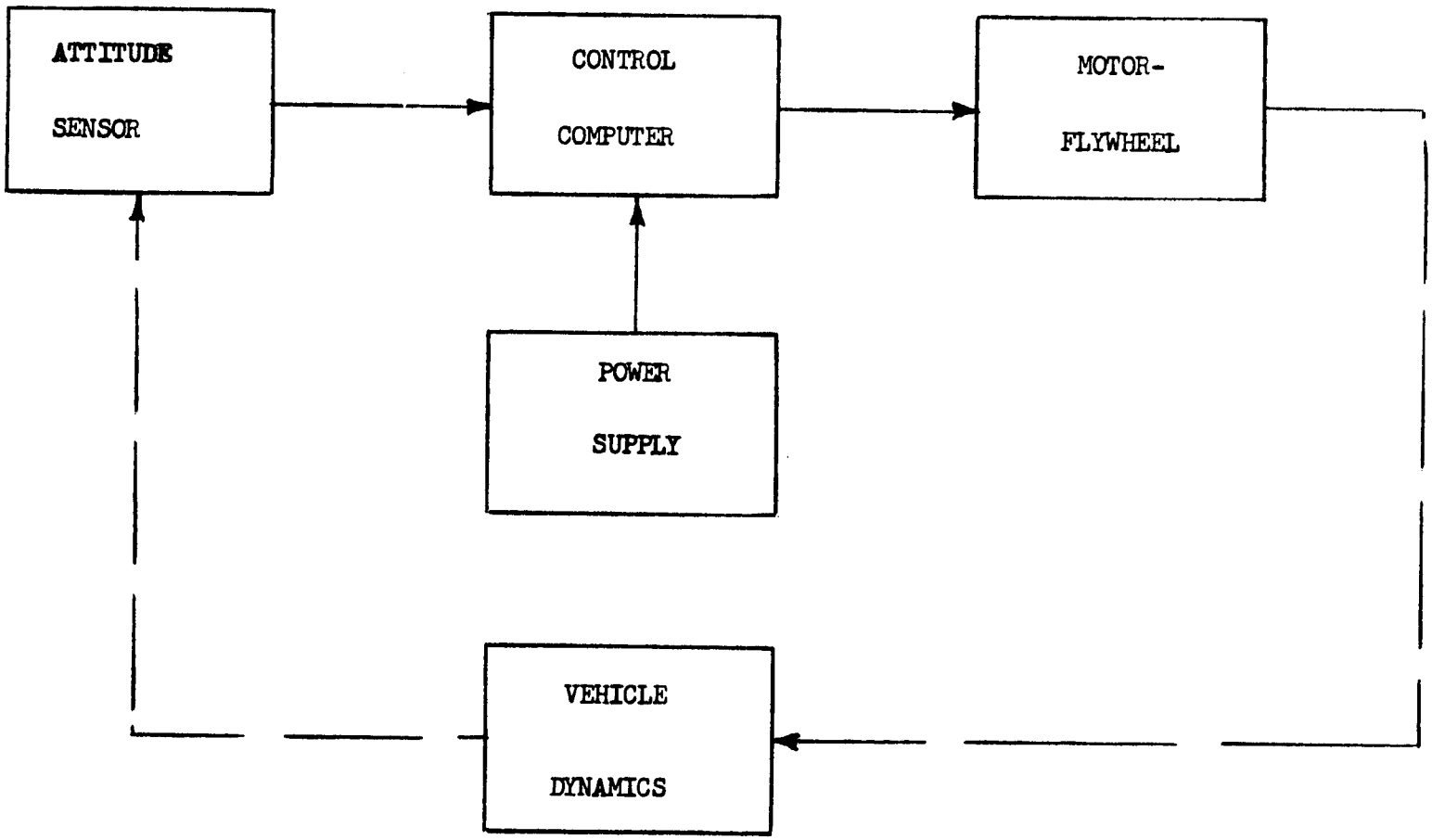

Fig. 1. FLYWHEEL CONTROL SYSTEM
(one axis)

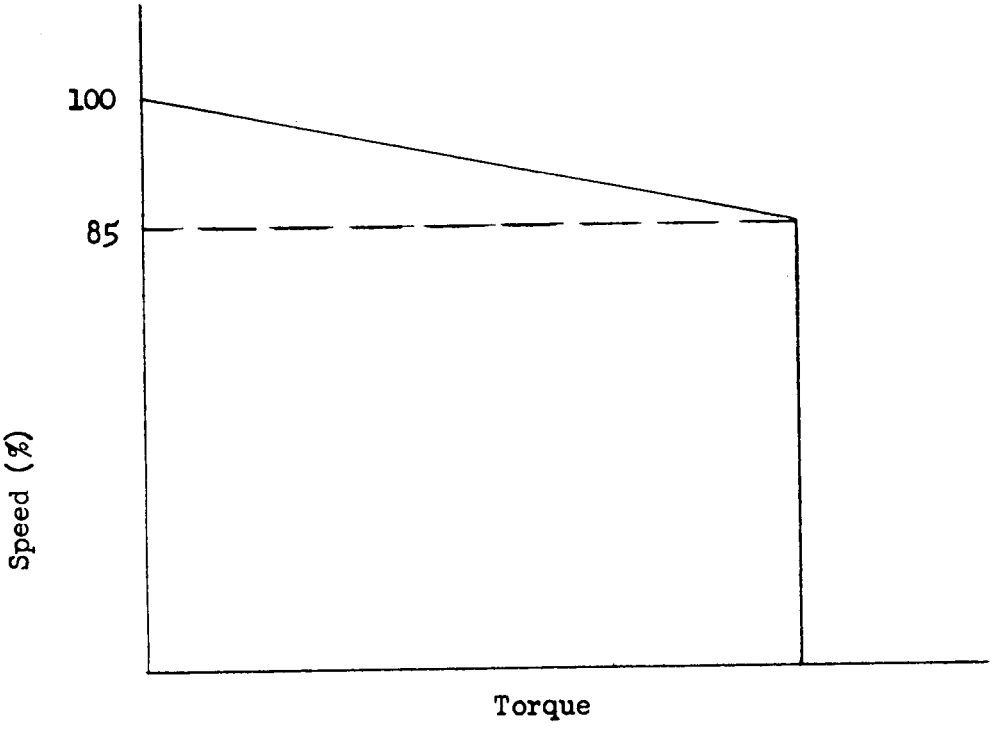

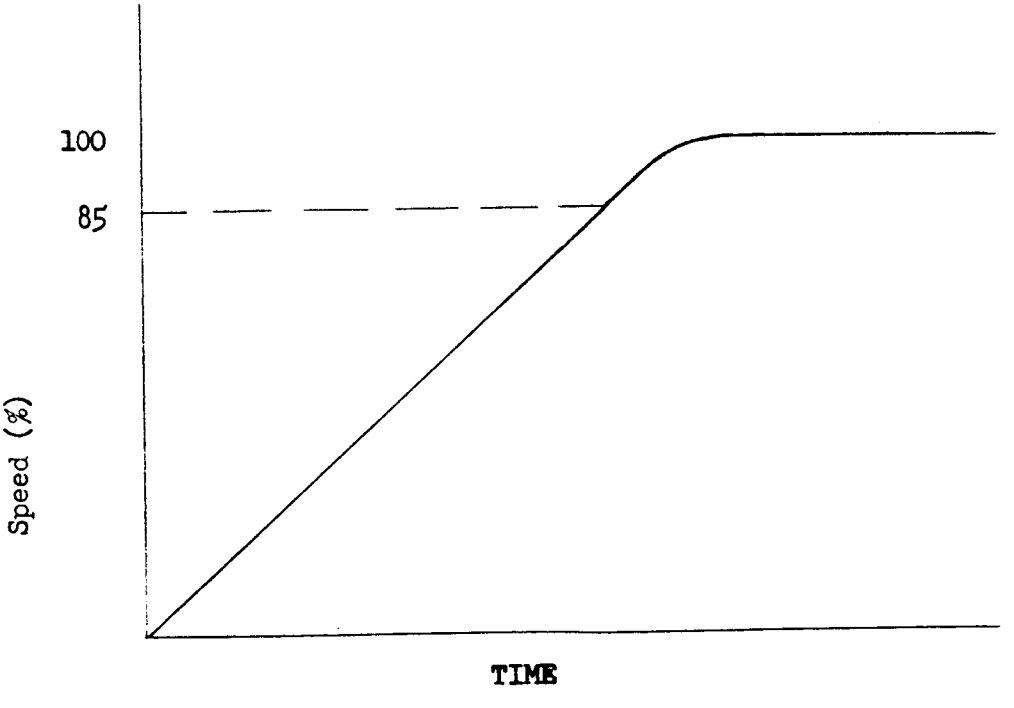

Fig. 2. MOTOR CHARACTERISTICS

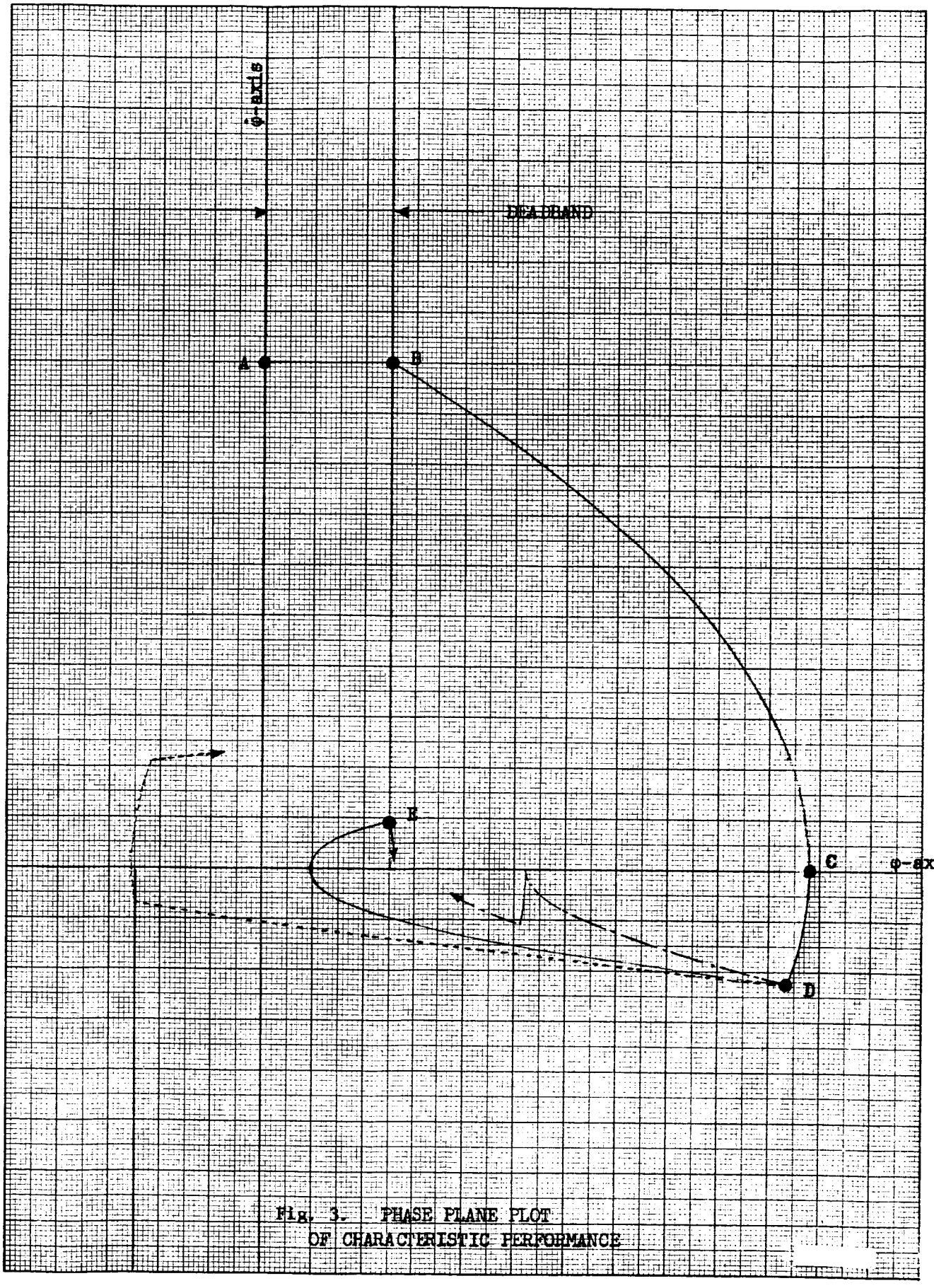

Fig. 3. PHASE PLANE PLOT
OF CHARACTERISTIC PERFORMANCE

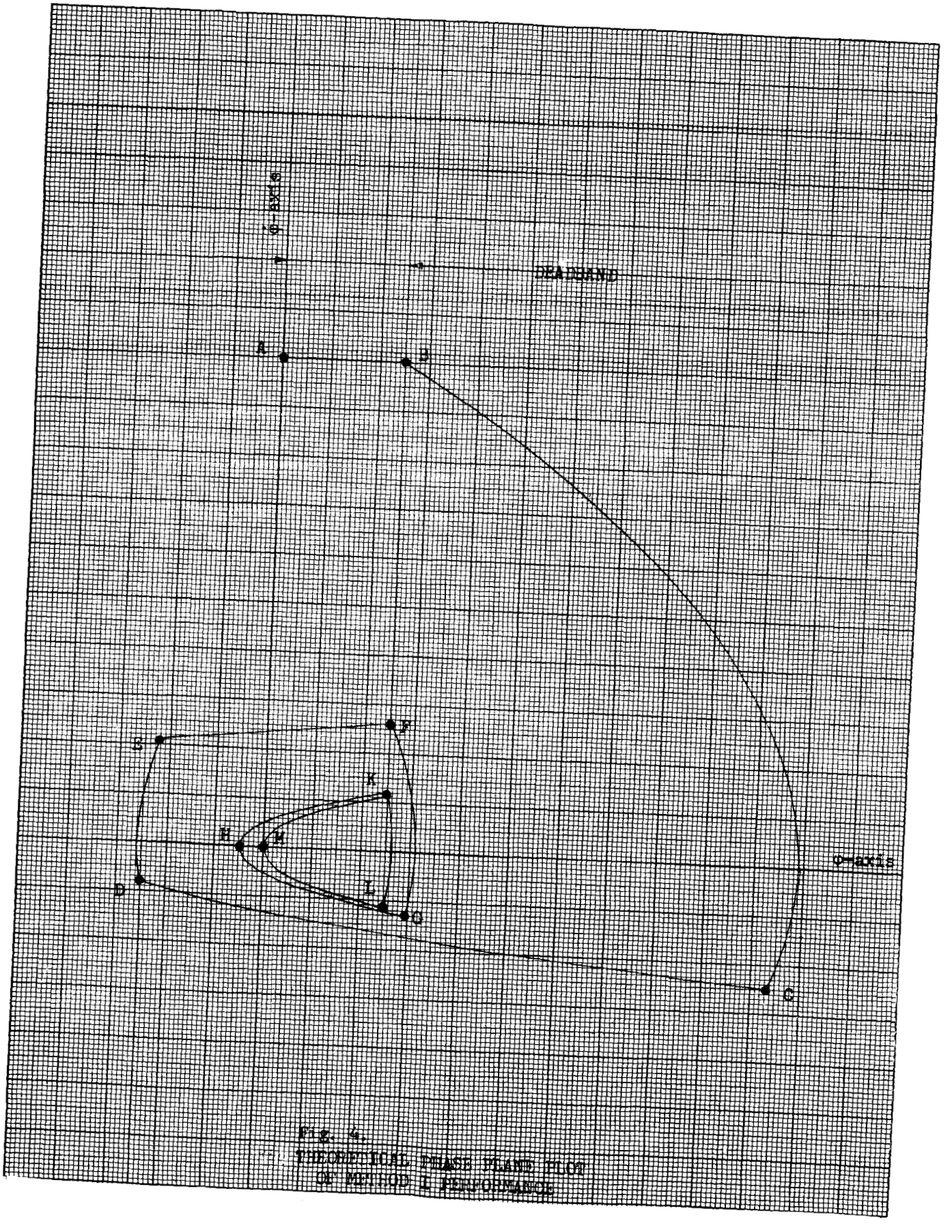

Fig. 4.
THEORETICAL PHASE PLANE PLOT
OF METHOD I PERFORMANCE

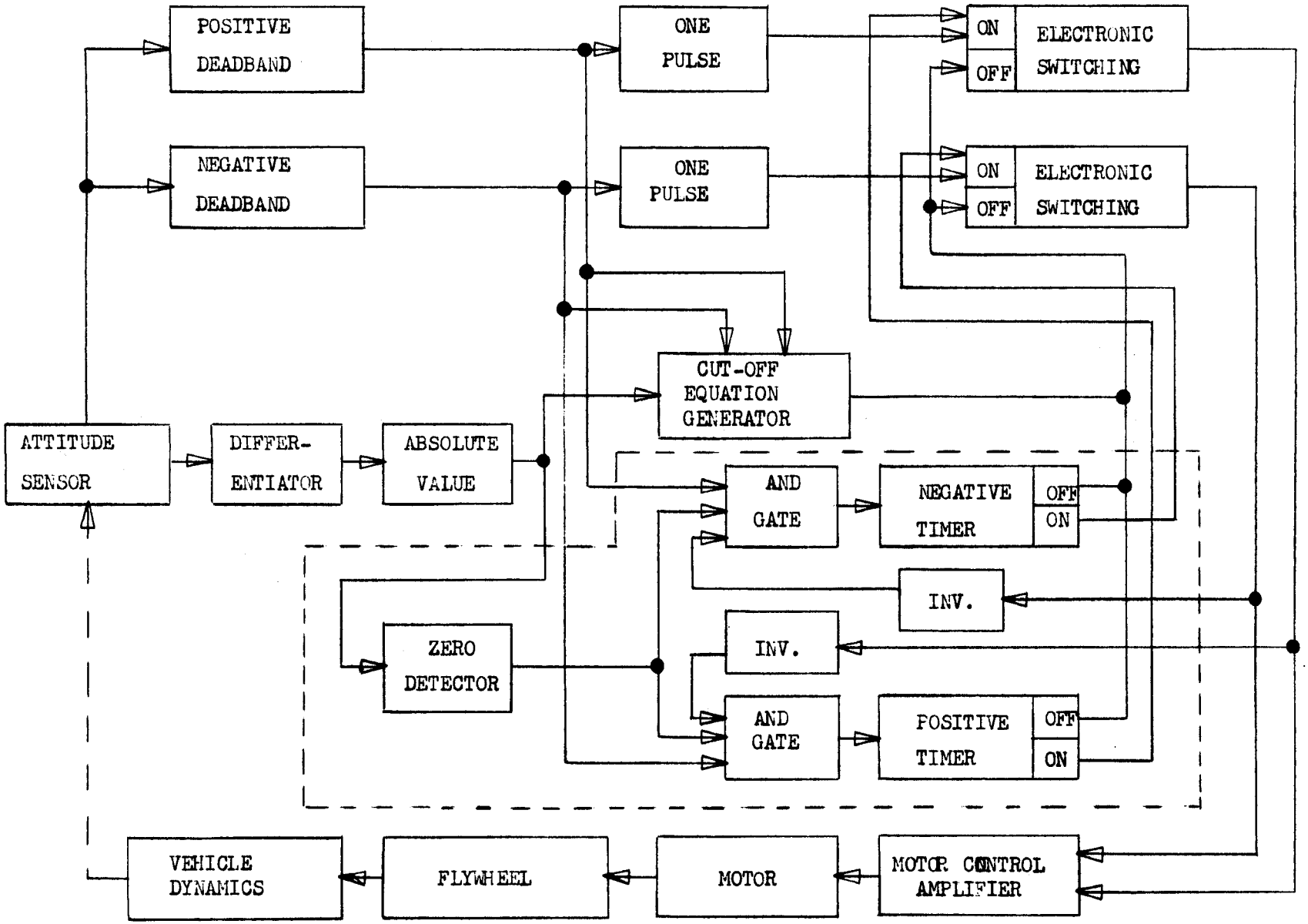

Fig. 5. BLOCK DIAGRAM OF METHOD I
(one axis)

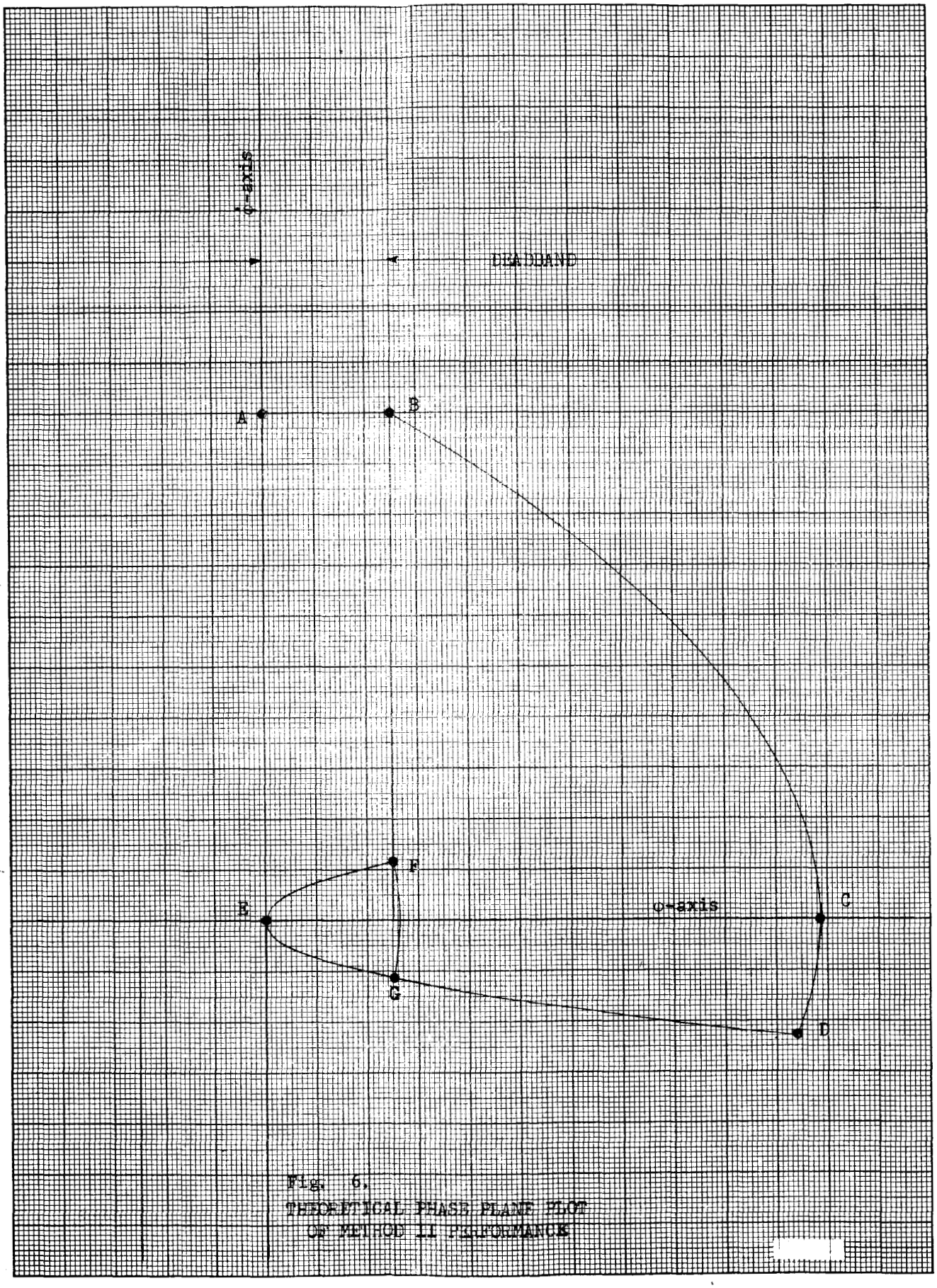

Fig. 6.
THEORETICAL PHASE PLANE PLOT
OF METHOD II PERFORMANCE

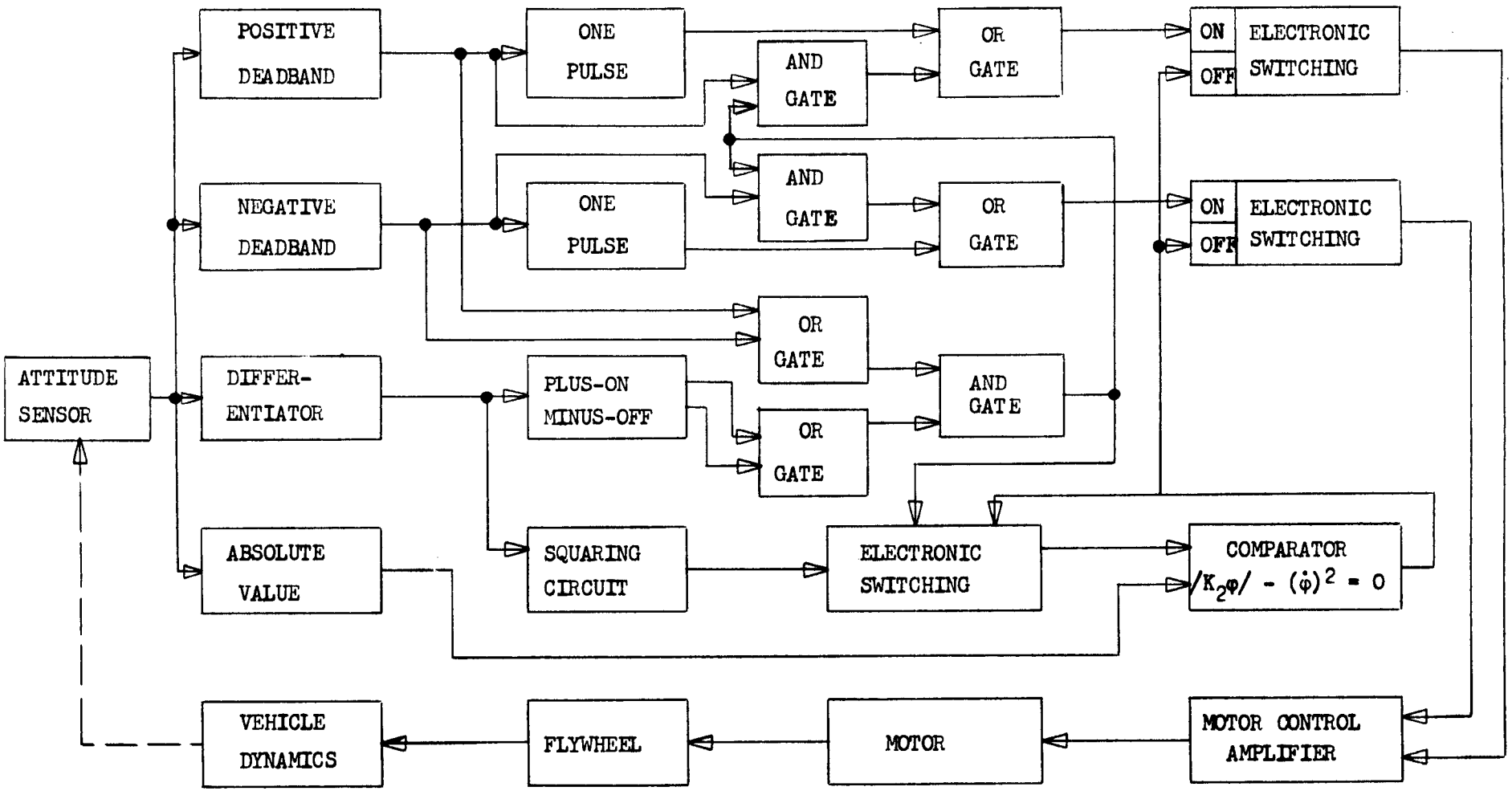

Fig. 7. BLOCK DIAGRAM OF SYSTEM II
(one axis)

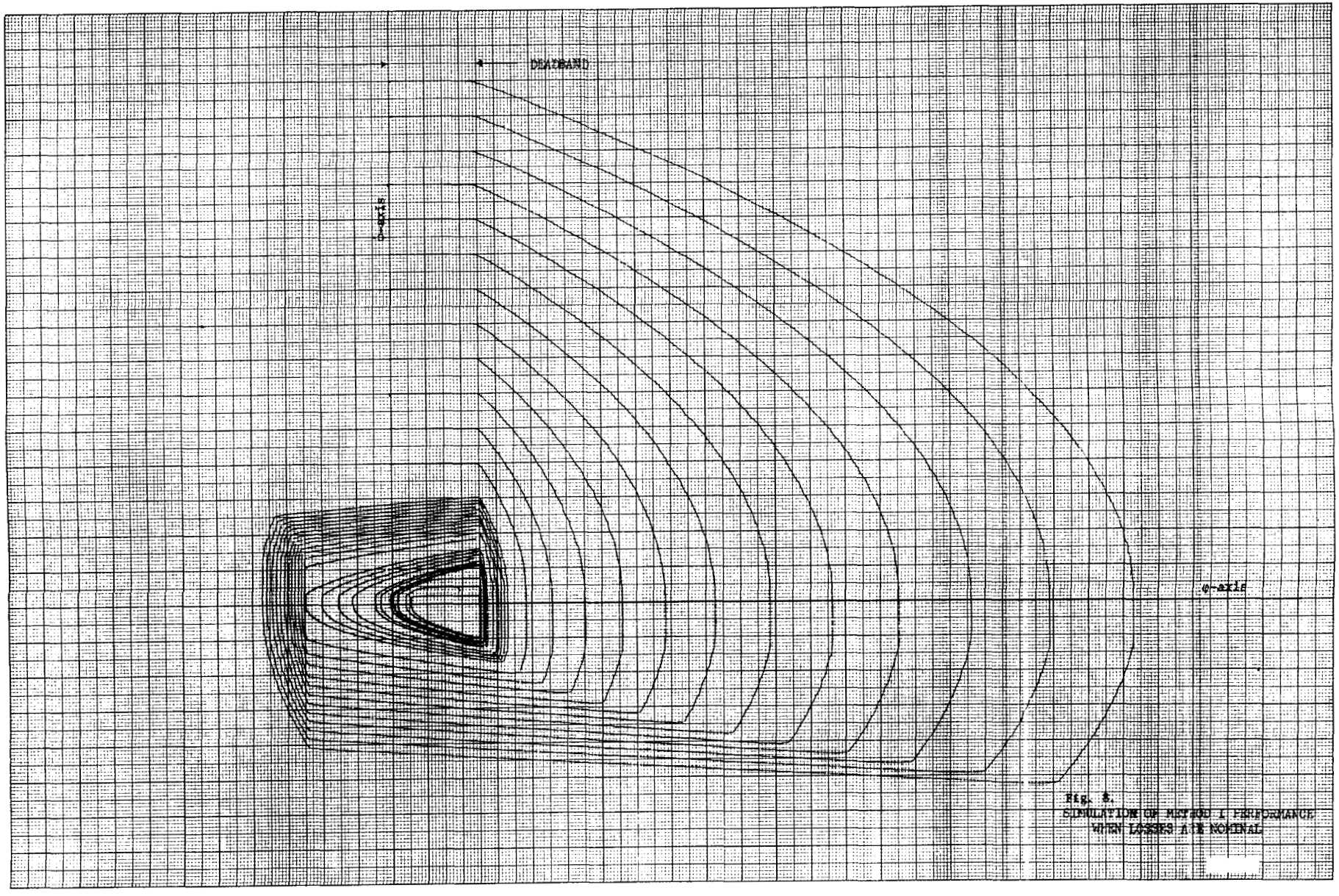

Fig. 8.
SIMULATION OF METHOD I PERFORMANCE
WHEN LOSSES ARE NOMINAL

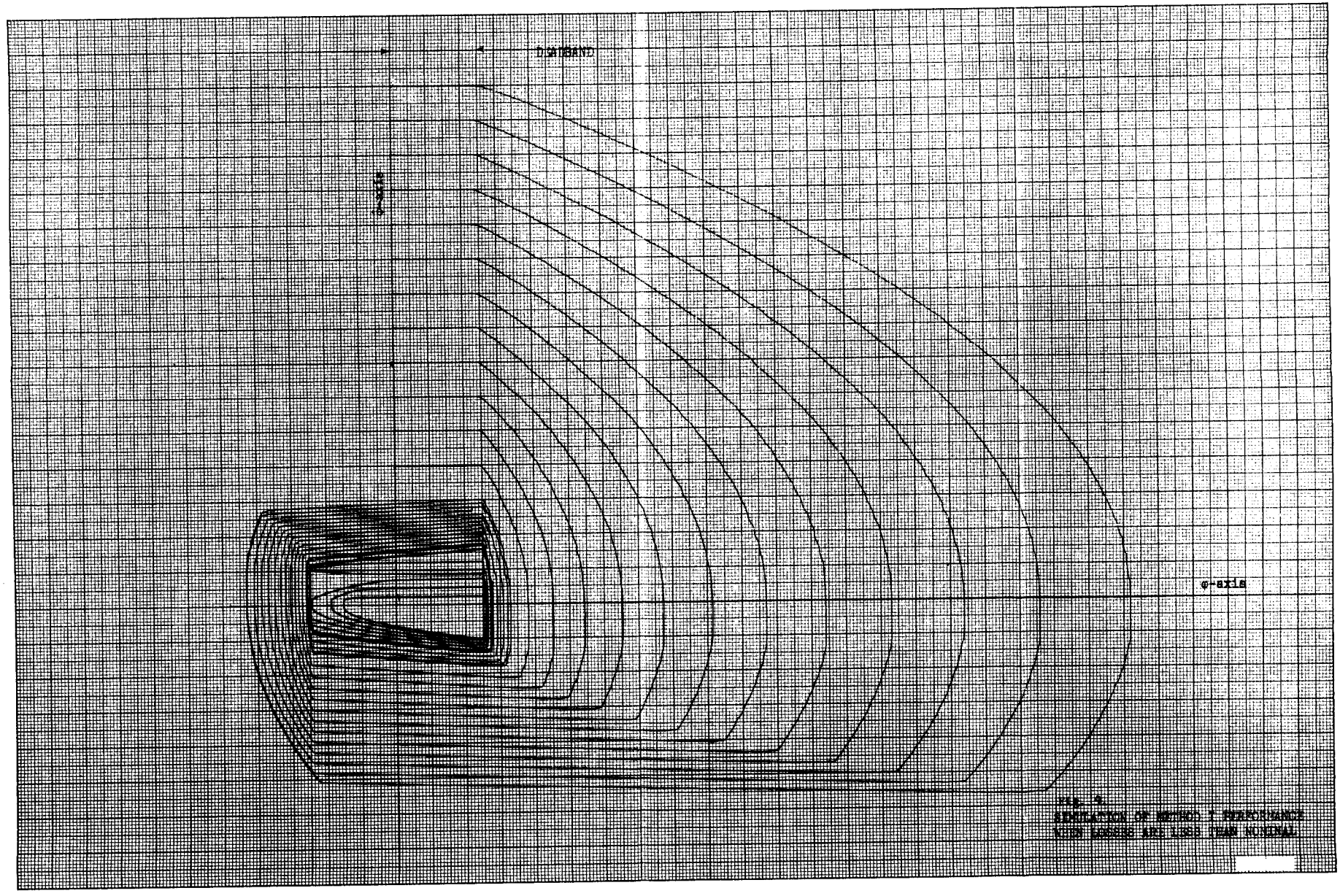

FIG. 4
SIMULATION OF METHOD 1 PERFORMANCE
WITH DOGBONE ARC LESS THAN NOMINAL

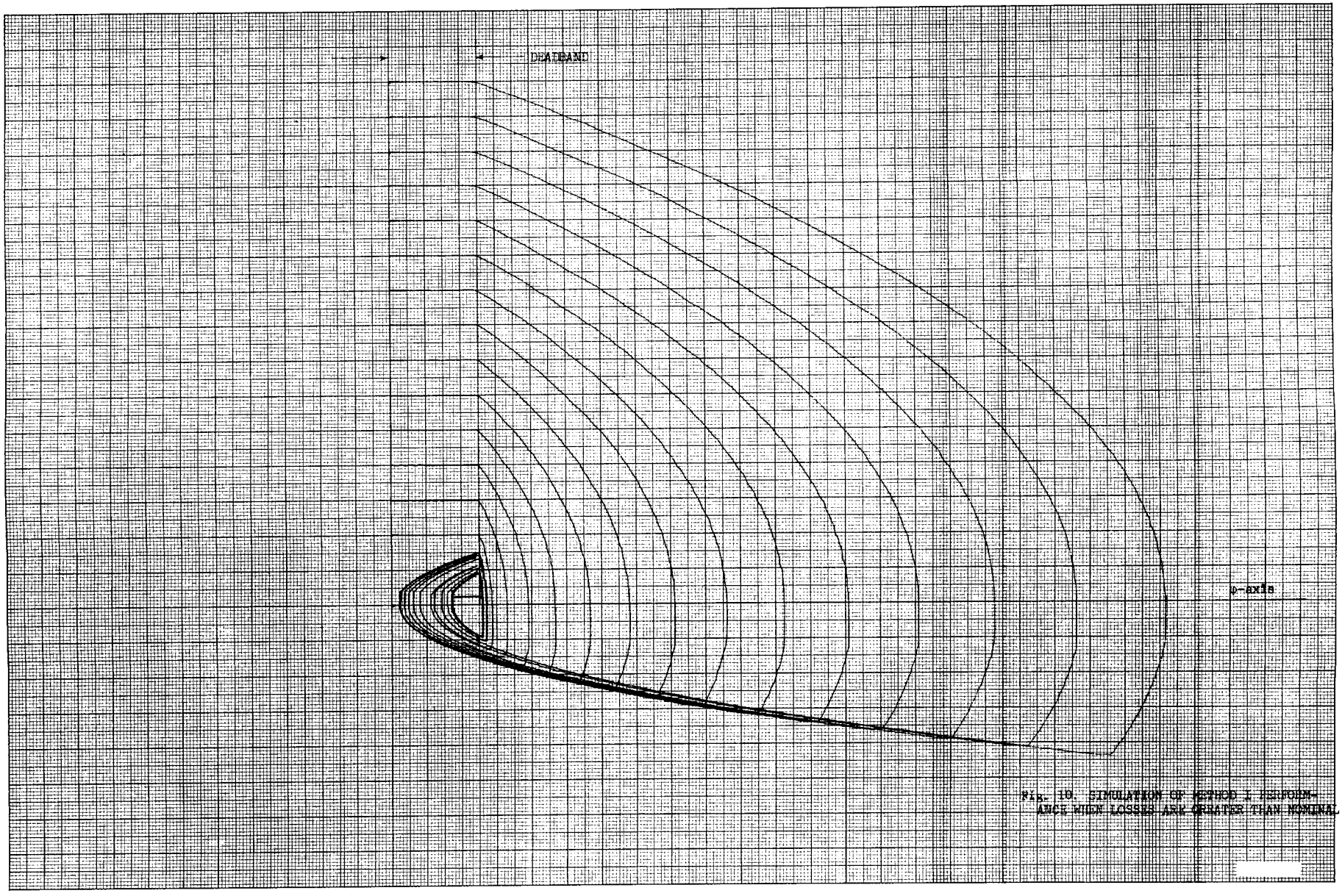

FIG. 10. SIMULATION OF METHOD I PERFORMANCE WHEN LOSSES ARE GREATER THAN NOMINAL

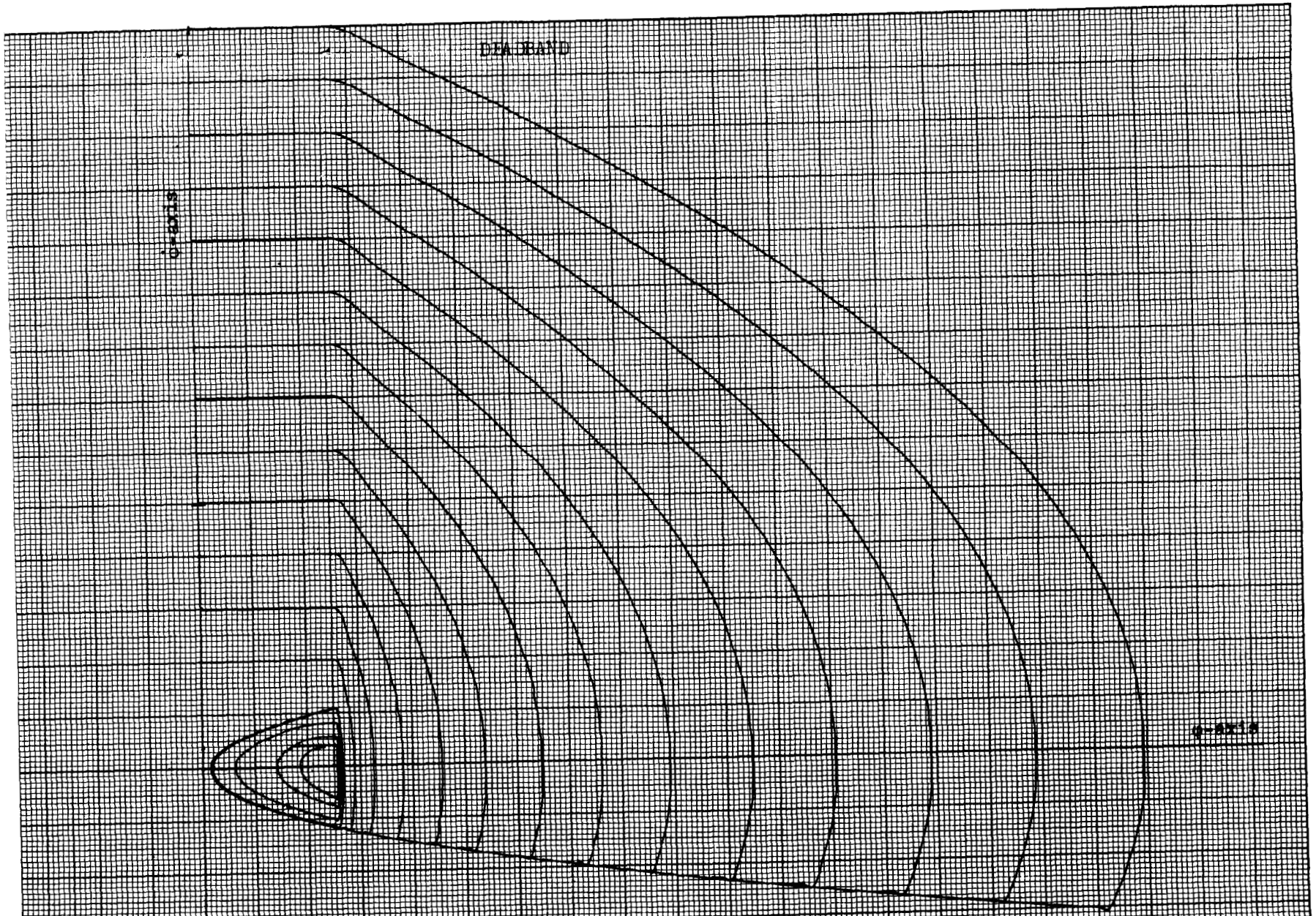

FIG. 11. SIMULATION OF METHOD II PERFORMANCE WHEN LOSSES ARE NOMINAL

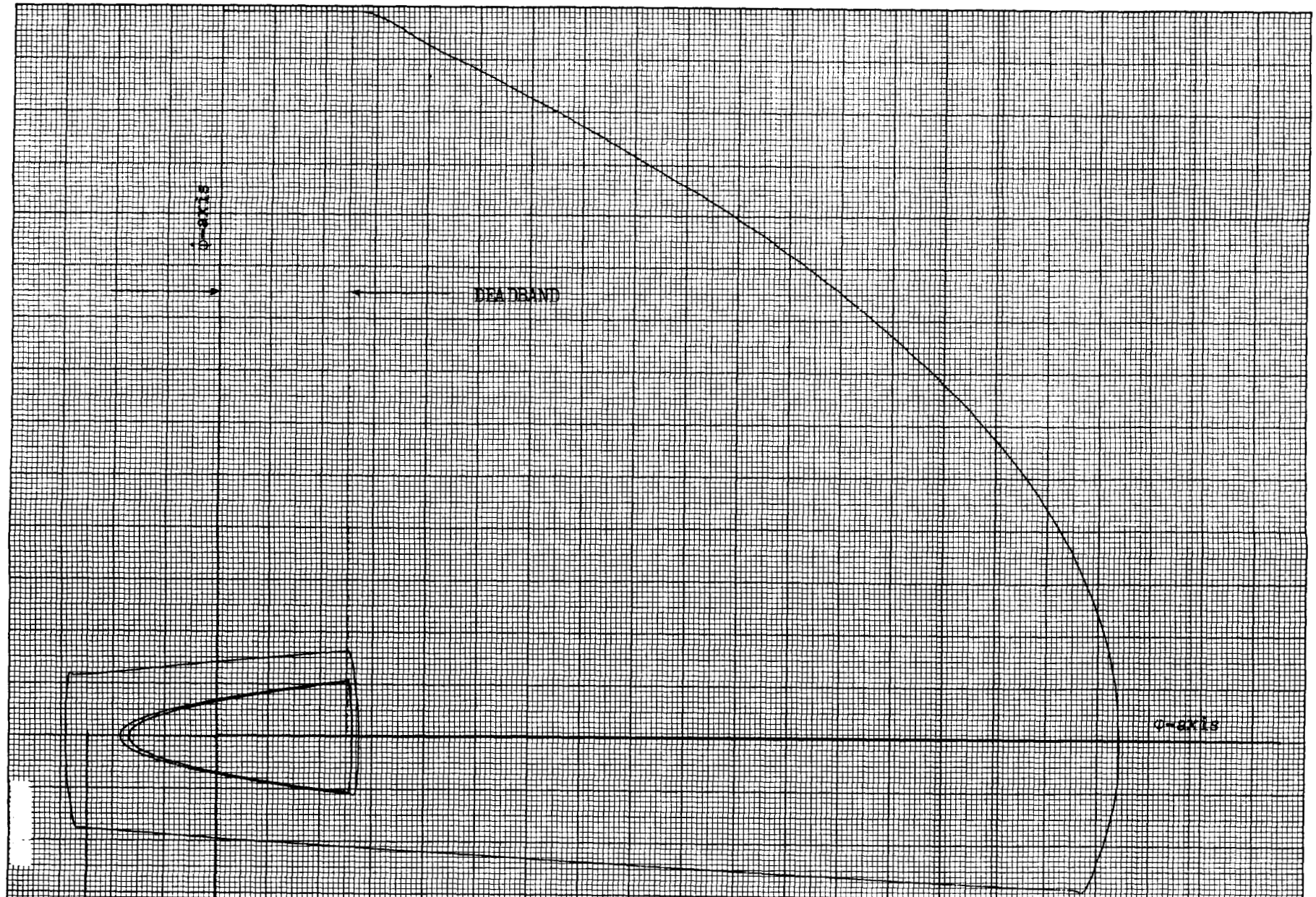

Fig. 12. SIMULATION OF METHOD II PERFORMANCE WHEN LOSSES ARE LESS THAN NOMINAL

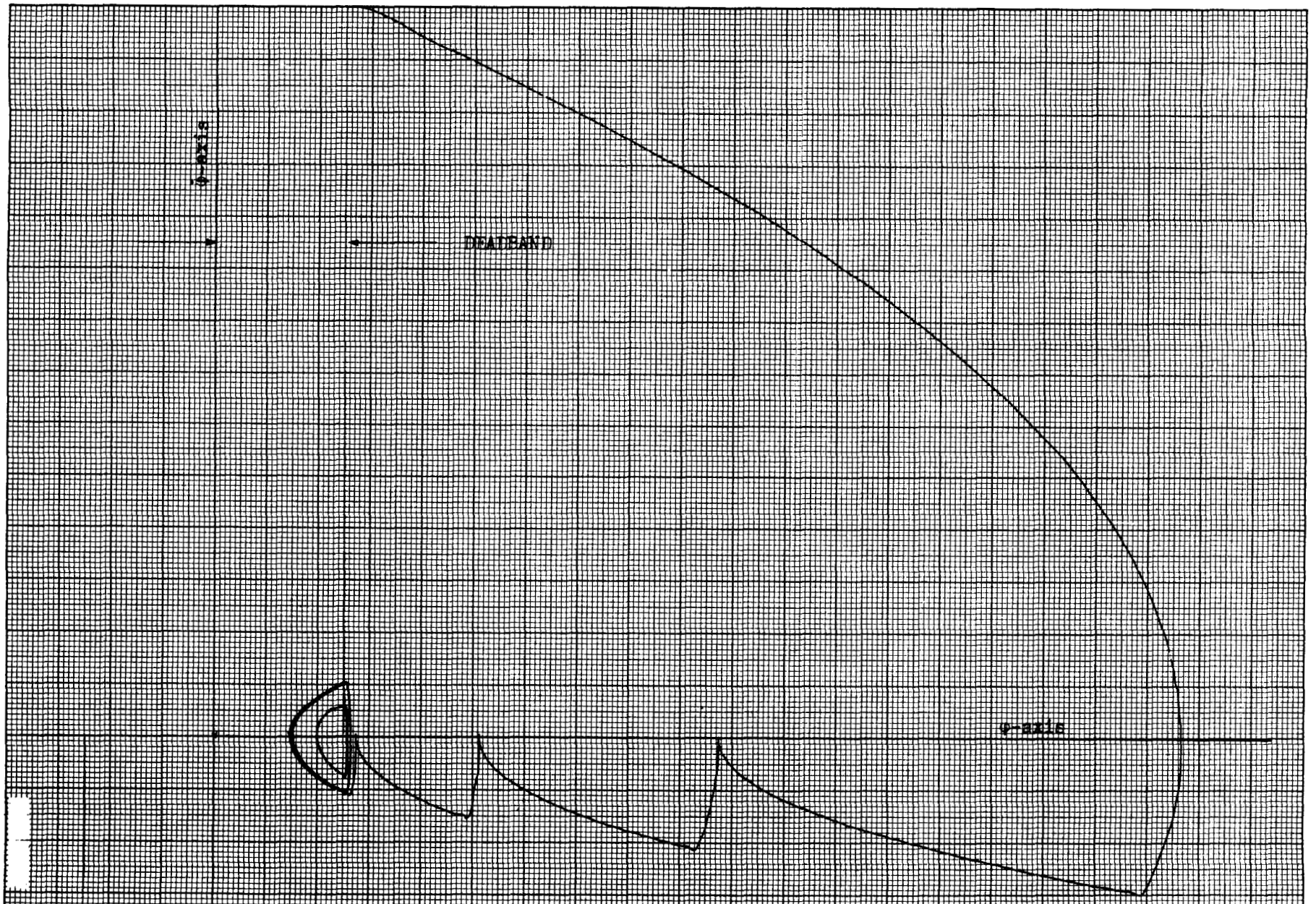

Fig. 13. SIMULATION OF METHOD II PERFORMANCE WHEN LOSSES ARE GREATER THAN NOMINAL

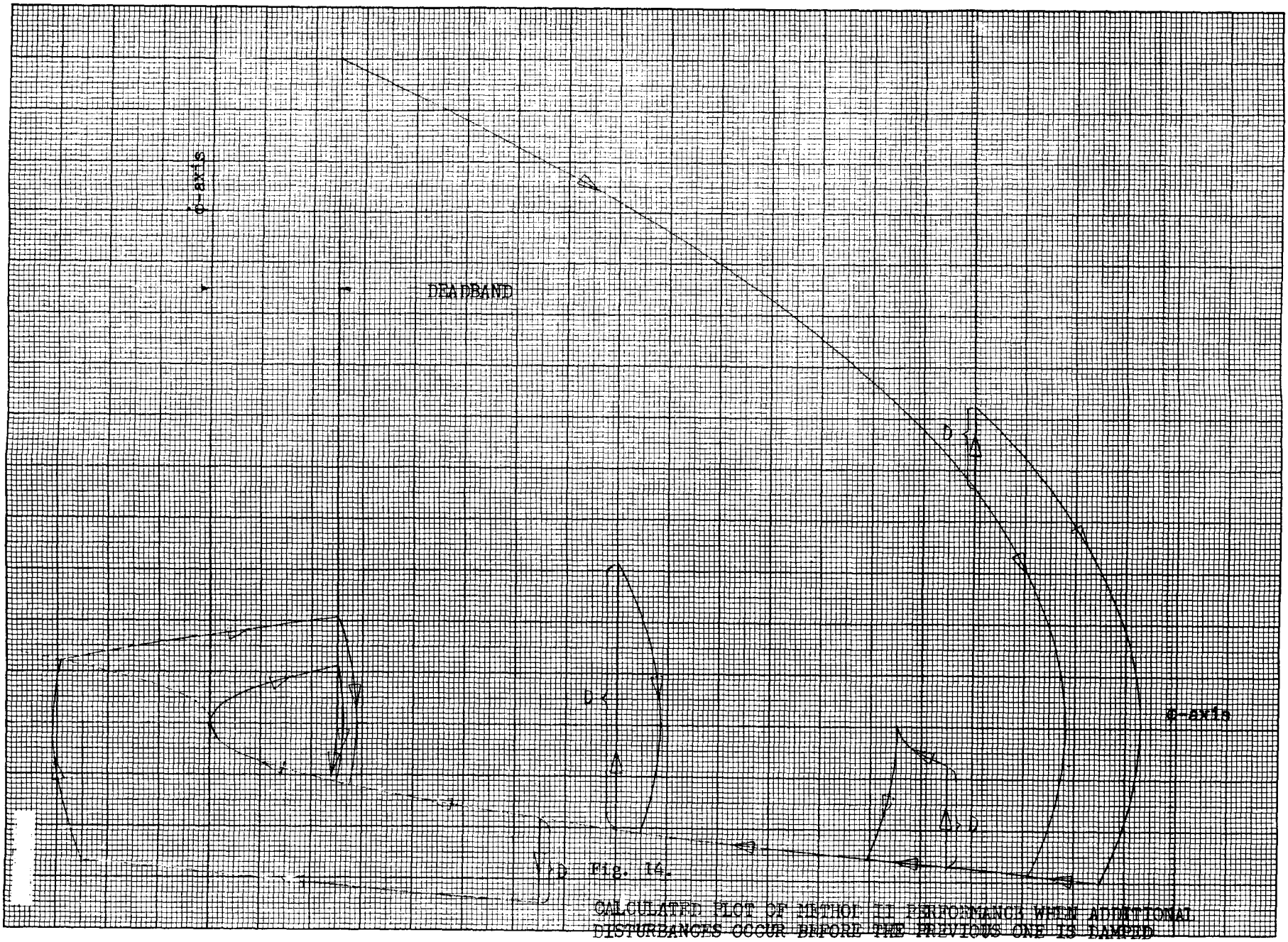

Fig. 14.

CALCULATED PLOT OF METHOD II PERFORMANCE WHEN ADDITIONAL DISTURBANCES OCCUR BEFORE THE PREVIOUS ONE IS DAMPED

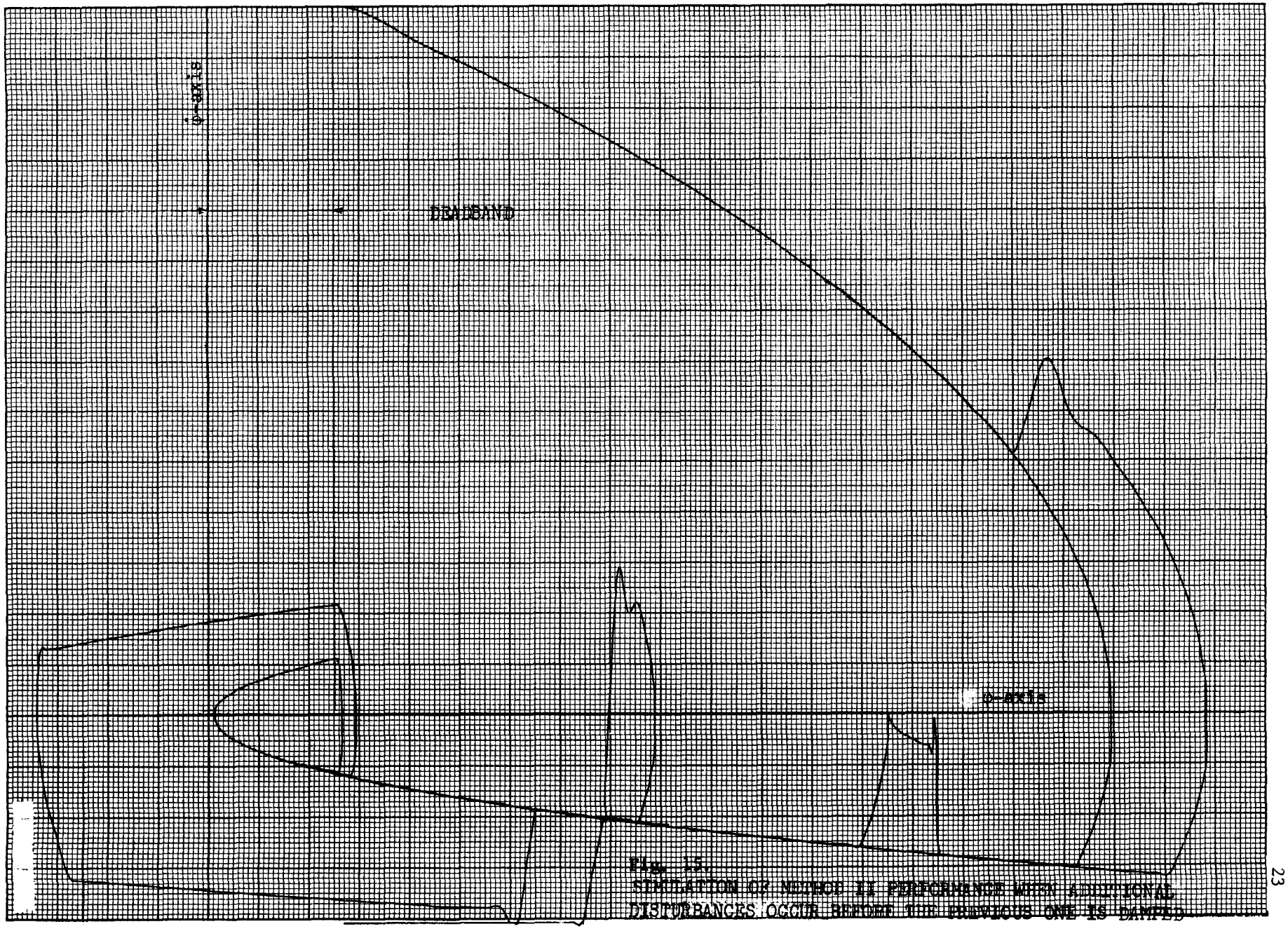

FIG. 15.
SIMULATION OF METHOD II PERFORMANCE WITH ADDITIONAL DISTURBANCES OCCUR BEFORE THE PREVIOUS ONE IS DAMPED

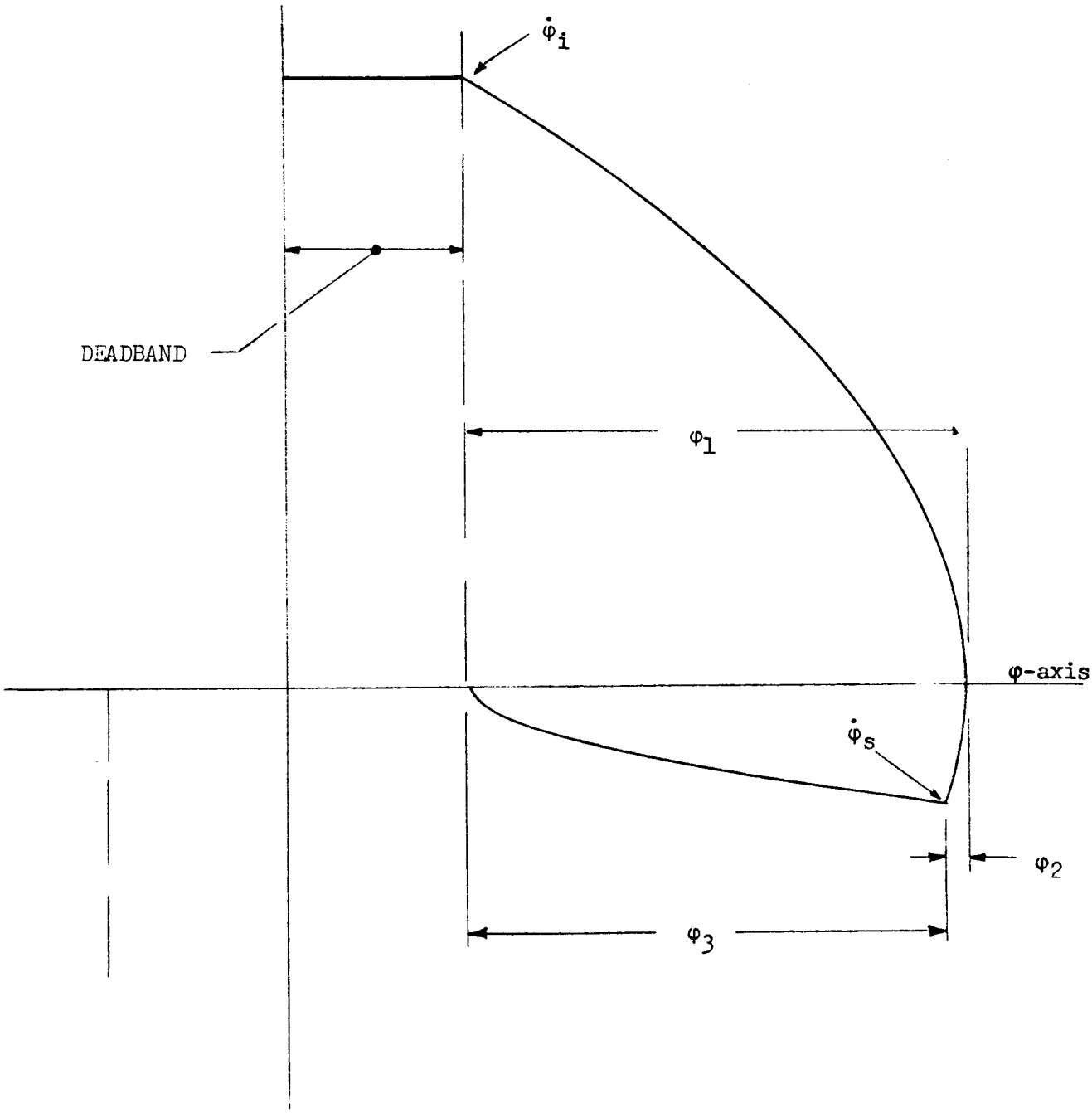

Fig. 16. DEFINITION OF DISPLACEMENTS

DISTRIBUTION:

M-DIR	Dr. von Braun
M-DEP-R&D	Mr. Rees
M-AERO-DIR	Dr. Geissler
M-G&C-F	Mr. Hosenthein (2)
M-G&C-A	Mr. Digesu
	Mr. deFries
M-G&C-M	Mr. Boehm
	Mr. Herrmann
M-G&C-R	Mr. Taylor
	Mr. Teuber
	Mr. Jurgensen
	Mr. Lacker
	Mr. Winkler
M-G&C-DIR	Dr. Haeussermann
M-G&C-N	Mr. Moore
	Mr. Richards
	Mr. Drawe
	Mr. Bridges
	Mr. Kennel (5)
	Mr. Golley (10)
M-MS-IP	Mr. Remer (8)